THE UNIVERSITY OF MICHIGAN

COLLEGE OF ENGINEERING
Department of Civil Engineering
Department of Aerospace Engineering

Technical Report

A NOTE ON THE PENETRATION OF A RIGID WEDGE INTO A NONISOTROPIC BRITTLE MATERIAL

Rafael Benjumea
David L. Sikarskie

ORA Project 01052

supported by:

DEPARTMENT OF THE INTERIOR
BUREAU OF MINES
GRANT NO. MIN-10
WASHINGTON, D.C.

administered through:

OFFICE OF RESEARCH ADMINISTRATION ANN ARBOR

September 1968

UMI 313

ABSTRACT

In the present note an existing wedge penetration theory for isotropic brittle materials is extended to explain some "bedding plane" effects observed in a series of experiments on Indiana limestone.

The general features of the theory presented in Reference [1] are kept here and in order to extend the analysis to the anisotropic case Jaeger's modification of the Coulomb-Mohr failure criteria is used.

Two specific cases of bedding plane orientation are considered, namely those in which the bedding planes are parallel and perpendicular to the direction of penetration.

The theory presented gives an insight into the anisotropic effects and predicts, in reasonable agreement with the experimental results, the observed differences in specific energies for the different penetration directions.

LIST OF SYMBOLS AND UNITS

d_i = penetration in the i^{th} cycle (in.)

d_i^* = penetration at the formation of the i^{th} chip (in.)

$\bar{E}_a$ = energy density for constant rate test (lb/in.^{2})

$\bar{E}_b$ = energy density for constant load test (lb/in.^{2})

k = slope of the force-penetration curve during crushing (lb/in.^{2})

K = slope of line connecting peak forces (lb/in.^{2})

L = length of fracture path (in.)

N = force normal to the fracture surface (lb/in.)

P_i = wedge force during the i^{th} cycle (lb/in.)

P_i^* = wedge force at the formation of the i^{th} chip (lb/in.)

S_1, S_2 = shear constants of the material (lb/in.^{2})

S_{c_1}, S_{c_2} = compressive strength of the material in two directions (lb/in.^{2})

T = force tangential to fracture surface (lb/in.)

ψ = failure angle of the chip

θ = one half of the wedge angle

γ = angle the bedding plane makes with the horizontal

ϕ = angle of internal friction (material constant)

σ = normal stress on fracture surface (lb/in.^{2})

τ = tangential stress on fracture surface (lb/in.^{2})

$\bar{\sigma}$ = normal stress average along the fracture surface (lb/in.^{2})

$\bar{\tau}$ = tangential stress average along the fracture surface (lb/in.^{2})

μ = related to ϕ by $\mu = \tan \phi$

I. Introduction

In the present Note an existing wedge penetration theory for brittle materials [1] is extended in an attempt to explain some "bedding plane" effects observed in a series of experiments on Indiana limestone. Bedding plane effect or rock anisotropy is often neglected in Rock Mechanics calculations particularly for rocks such as Indiana limestone where there is no discernible bedding plane and further the change in physical properties, e.g., compressive strength, with direction is relatively small. The present theory (substantiated by experiment) indicates, however, that relatively large differences in the specific energy (energy necessary to remove a unit volume of rock) can exist even for relatively small anisotropy.

The analysis presented herein follows that of [1] and contains the same basic assumptions. The material behavior under consideration is typically brittle, i.e., as the wedge penetrates cycles of crushing followed by the formation of chips are experienced. To extend the analysis to the anisotropic case Jaeger's [2,3] modification of the Coulomb-Mohr failure criterion is used.

Two special cases are considered in this Note, namely $\gamma = 0°, 90°$, see Figure 1, where γ represents the angle the bedding plane makes with the horizontal. Intermediate values of γ represent a much more difficult problem since symmetry cannot be invoked. This necessitates some description of the wedge kinematics.

In the following section theoretical results are derived. A comparison of the theory with some previously unpublished [4] wedge penetration experi-

ments on Indiana limestone is given in section III followed by a discussion of results in section IV.

II. Theoretical Analysis

Figure 2 illustrates the assumed idealized penetration model just at the formation of the $(i+1)^{st}$ chip. Chip failure is assumed planar and inclined to the horizontal at some as yet unknown angle ψ. Considering equilibrium just before formation of the chip gives the following for the normal and tangential forces on the failure plane[1];

$$N = \frac{P^*_{i+1}}{2} \frac{\sin(\psi+\theta)}{\sin\theta} \tag{1}$$

$$T = \frac{P^*_{i+1}}{2} \frac{\cos(\psi+\theta)}{\sin\theta} \tag{2}$$

where

P^*_{i+1} = force per unit length of cutting edge necessary to remove the $(i+1)^{st}$ chip

2θ = wedge angle

and N, T are resultant forces per unit length of cutting edge defined by,

$$N = \int_0^L \sigma(\xi)d\xi \quad ; \quad T = \int_0^L \tau(\xi)d\xi \tag{3}$$

where $\sigma(\xi)$, $\tau(\xi)$ are the normal and shear stress distributions along the failure plane, respectively. L is the chip length and can be expressed;

$$L = \frac{d^*_{i+1}}{\sin \psi} \tag{4}$$

where d^*_{i+1} is the penetration at the $(i+1)^{st}$ chip removal.

The Coulomb-Mohr failure criterion [2,3], modified to account for rock anisotropy, is given by[2];

$$|\tau| - \tan \phi \, \sigma - [S_1 - S_2 \cos 2(\psi - \gamma)] = 0 \tag{5}$$

where

ϕ = angle of internal friction (assumed constant throughout)

S_1, S_2 = material constants.

The angle $(\psi - \gamma)$ measures the angle between the plane of minimum shear strength (bedding plane in this case) and the plane of failure. Note that the maximum and minimum shear strengths are 90° apart and are S_1+S_2, S_1-S_2, respectively. The analysis further assumes that, to a first approximation, the failure criterion is satisfied everywhere along the failure plane. Equation (4) can thus be integrated over the length L and a stress averaged form of the failure criterion used

i.e., $$|\bar{\tau}| - \tan \phi \, \bar{\sigma} - [S_1 - S_2 \cos 2(\psi - \gamma)] = 0 \tag{6}$$

where

$$\bar{\sigma} = \frac{N}{L} \quad ; \quad \bar{\tau} = \frac{T}{L}$$

Using equations (1), (2), and (4), equation (6) can be expressed,

$$\frac{P^*_{i+1}}{2d^*_{i+1}} \frac{\sin\psi\cos(\psi+\theta+\phi)}{\sin\theta\cos\phi} - [S_1 - S_2\cos 2(\psi-\gamma)] = 0 \qquad (7)$$

Failure will occur at that angle ψ such that the left-hand side of equation (7) has a maximum value. This is found by considering $\frac{d(\text{L.H.S.})}{d\psi} = 0$, with the result;

$$\tan 2\psi = \frac{\frac{P^*_{i+1}}{d^*_{i+1}}\cos(\theta+\phi)+4S_2\sin 2\gamma\cos\phi\sin\theta}{\frac{P^*_{i+1}}{d^*_{i+1}}\sin(\theta+\phi)+4S_2\cos 2\gamma\cos\phi\sin\theta} \qquad (8)$$

The ratio P^*_{i+1}/d^*_{i+1} is still unknown, however. Substituting equation (8) into equation (7), the following quadratic equation in P^*_{i+1}/d^*_{i+1} results.[3]

$$\left(\frac{P^*_{i+1}}{d^*_{i+1}}\right)^2\cos^2(\phi+\theta) - 8\sin\theta\cos\phi[S_1\sin(\phi+\theta)-S_2\sin(2\gamma+\theta+\phi)]\left(\frac{P^*_{i+1}}{d^*_{i+1}}\right)$$
$$- 16\sin^2\theta\cos^2\phi[S_1^2-S_2^2] = 0 \qquad (9)$$

Just as in the isotropic case P^*_{i+1}/d^*_{i+1} is a constant, K, for all i, dependent only on the parameters and material properties. Note that equation (9) gives the isotropic results for $S_2 = 0$, see [1]. The positive root of equation (9) is the correct one, see Appendix A

$$\frac{P^*_{i+1}}{d^*_{i+1}} = \frac{4 \sin\theta \cos\phi}{\cos^2(\theta+\phi)}\Big\{ S_1 \sin(\theta+\phi) - S_2 \sin(2\gamma+\theta+\phi) + \sqrt{[S_1 \sin(\theta+\phi) - S_2 \sin(2\gamma+\theta+\phi)]^2 + [S_1^2 - S_2^2]\cos^2(\theta+\phi)}\Big\} = K \tag{10}$$

From equation (10) the ratio of load to penetration at chip formation is now known, however, the individual magnitudes of P^*_{i+1} and d^*_{i+1} are not. An additional equation is available, however, namely the crushing law.[4]

$$P_{i+1} = k[d_{i+1} - d^*_i] \tag{11}$$

where k is material constant dependent, in addition, on wedge geometry and direction of penetration. At the time of chip formation equation (11) becomes

$$P^*_{i+1} = k[d^*_{i+1} - d^*_i] \tag{12}$$

Following [1], equations (10) and (12) can be solved simultaneously to obtain P^*_{i+1}, d^*_{i+1} in terms of d^*_i. Recurrence relations can then be derived which relate P^*_{i+n}, d^*_{i+n} to d^*_i.

i.e.,

$$P^*_{i+n} = K\left(\frac{k}{k-K}\right)^n d^*_i$$

$$d^*_{i+n} = \left(\frac{k}{k-K}\right)^n d^*_i \tag{13}$$

Thus, for i = 1, the force and penetration levels after n cycles can be related

to the penetration at the first chip. Note that geometric similarity exists (due to linearity) with the similarity variable $\frac{k}{k-K}$. In Figure 3 the actual penetration process is shown along with two idealizations (constant rate, constant load tests) which bound the actual.

Determination of the specific energy (energy required per unit volume of rock removed) for the constant rate, constant load tests follows the analysis of [1] exactly. It should be noted that only for the special cases included in this Note ($\gamma = 0, 90°$) (symmetric cases) will the analysis be the same. The specific energies for the constant rate test and constant load test are obtained by dividing the energy consumed in each test, see Figure 4, by the volume removed and are respectively;

$$\bar{E}_a = \frac{kK}{2(2k-K)} \tan \psi \tag{14}$$

$$\bar{E}_b = \frac{K[(k-K)^2+k^2]}{2k(2k-K)} \tan \psi \tag{15}$$

In the following section numerical results are compared with some experiments on Indiana limestone.

III. Experimental and Numerical Results

The pertinent experimental results [4] for Indiana limestone are listed in Table I. For $\gamma = 0°, 90°$ the force is perpendicular and parallel to the bedding plane, respectively, for both the compressive strength and wedge penetration tests.

The compressive strength tests were conducted on cylinders 1.75 in. in

diameter and 4.75 in. long. Sample ends were finished to a tolerance of ± .005 in. and during tests were directly in contact with the platen (unlubricated).

All of the wedge-penetration experiments were run with a tungsten carbide wedge having a 1 in. cutting edge, a wedge angle of $2\theta = 90°$, and a tip radius of .05 in. Maximum penetration depths of the order .15 in. were run. The rock sample was a cube approximately 12 in. on a side. Force, penetration results were taken out directly on an x-y plotter and measurements of crushing slope, envelope slope, and energy were computed from the graphs. Crater volumes were obtained using a burette. The craters were first coated to prevent absorption and several readings were then averaged.

As input for the numerical results, the following items are needed: k, 2θ, ϕ, S_1, and S_2. k will be taken from the experimental results. The wedge angle is, $2\theta = 90°$. The angle of internal friction ϕ is difficult to establish, particularly in the vicinity of the wedge tip where the mean or hydrostatic stress can be extremely high. In any event, numerical values are computed for three different values of ϕ[5]: ($\phi = 5°, 10°, 20°$). S_1 and S_2 can be found from the following equations, see Appendix B;

$$4[S_1^2-S_2^2] + 4[S_1+S_2]\mu\, S_{c_1} = S_{c_1}^2$$

$$4[S_1^2-S_2^2] + 4[S_1-S_2)\mu\, S_{c_2} = S_{c_2}^2 \qquad (16)$$

where

S_{c_1} = compressive strength for $\gamma = 0°$

S_{c_2} = compressive strength for $\gamma = 90°$

$\mu = \tan \phi$

Numerical values for S_1, S_2 as a function of ϕ are given in Table II. Using equations (8), (10), (14), and (15), the chip failure angle, the slope of the envelope, and the specific energies for both cases can be computed for $\gamma = 0°$, $\gamma = 90°$. The results are presented in Table III.

These results are discussed and compared with the experimental data in the following section.

IV. Discussion of Results

The experimental results for Indiana limestone illustrated in Table I, indicate a rather interesting behavior; namely, a much larger difference in specific energy in perpendicular directions than in the corresponding material properties. An extension of an existing theory has been outlined herein which predicts at least qualitatively the same trends, see Table III. Several problems exist. While the trends are established, a large amount of scatter was evident in the experimental results. The numbers presented represent a simple average of available data. Concerning the theory, it should be pointed out that not all input data (material properties) is clearly established, e.g., the angle of internal friction ϕ. Two major drawbacks of the theory are the assumptions made in the analysis and the inability of the theory to adequately describe the initial phases of the penetration process. These questions are discussed in more detail in Reference [1]. In spite of this, however, the theory is in good agreement qualitatively, i.e., it provides an explanation of

the difference in specific energies in the two directions. It is also felt that quantitative agreement is reasonable in view of the statistical nature of the material, and the simplifying assumptions of the analysis.

From Table III it is evident that the numerical results are very sensitive to the angle of internal friction ϕ. Comparing Tables I and III for ϕ = 10° indicates that the computed envelope slope is in good agreement with the experimental value. This is some what inconclusive, however, due to the limited test data. Concerning the specific energies, although the same trends exist in the numerical data for γ = 0°, 90°, the numerical results are uniformly higher than the experimental. For ϕ = 10°, the experimental value of the specific energy lies outside the "bounds." It is felt that this is due to the assumption of the failure criterion being satisfied along the entire failure plane.

Several interesting features appear in the analysis. As anisotropy increases, i.e., as $S_{c_1} - S_{c_2}$ increases, it can be shown that the differences in the failure angle ψ and the specific energies for γ = 0°, γ = 90° also increases, as is expected. It is also interesting to note that the slope of the envelope is larger in the direction parallel to the bedding plane. This indicates the possibility of wedge forces larger for penetrations parallel to the bedding than perpendicular (for equal penetration distances). This is opposite to the crushing phase where the crushing slope is largest perpendicular to the bedding plane. The physical difference in specific energies is also related to this question, i.e., since K is larger, k is smaller for γ = 90°, more energy is consumed in the penetration. Also, the failure angle is larger

for $\gamma = 90°$ leading to smaller volumes. Both of these effects lead to larger specific energies for $\gamma = 90°$.

Appendix A. Derivation of the Quadratic Equation in $\frac{P^*_{i+1}}{d^*_{i+1}}$

The failure criterion is given by equation (7) with the failure angle ψ defined by equation (8). If we further define,

$$K_1 = \frac{P^*_{i+1}}{2d^*_{i+1}} \frac{1}{\sin\theta \cos\phi} \tag{A1}$$

the failure criterion can be written in the following form

$$K_1 \sin\psi \cos(\phi+\theta+\psi) - [S_1 - S_2 \cos 2(\psi-\gamma)] = 0 \tag{A2}$$

expanding:

$$K_1[\sin 2\psi \cos(\theta+\phi) - \sin(\theta+\phi)(1-\cos 2\psi)]$$
$$-2[S_1 - S_2(\cos 2\gamma \cos 2\psi + \sin 2\gamma \sin 2\psi)] = 0 \tag{A3}$$

Dividing by cos 2ψ and collecting terms;

$$[K_1 \cos(\theta+\phi) + 2S_2 \sin 2\gamma]\tan 2\psi$$
$$+ [K_1 \sin(\theta+\phi) + 2S_2 \cos 2\gamma] \tag{A4}$$
$$- [2S_1 + K_1 \sin(\theta+\phi)]\sqrt{1+\tan^2 2\psi} = 0$$

This has the form

$$A \tan 2\psi + B - C\sqrt{1 + \tan^2 2\psi} = 0 \tag{A5}$$

where A, B, and C can be determined from equation (A4). Note also, from

equation (8), that;

$$\tan 2\psi = \frac{A}{B} \tag{A6}$$

Substituting (A6) into (A5) we find:

$$A^2 + B^2 - C\sqrt{A^2+B^2} = 0$$

or[6]

$$A^2 + B^2 = C^2 \tag{A7}$$

Substituting back for A, B, C, and K_1, and rearranging, the final form results.

$$\left(\frac{P^*_{i+1}}{d^*_{i+1}}\right)^2 \cos^2(\theta+\phi) - 8 \sin\theta \cos\phi \,[S_1 \sin(\theta+\phi) - S_2 \sin(2\gamma+\theta+\phi)]\left(\frac{P^*_{i+1}}{d^*_{i+1}}\right)$$

$$- 16 \sin^2\theta \cos^2\phi [S_1^2 - S_2^2] = 0 \tag{A8}$$

This quadratic equation has a positive and a negative root. The negative root means the slope $\frac{P^*_{i+1}}{d^*_{i+1}}$ is negative which has no physical meaning.

Appendix B. Computation of the Shear Constants S_1, S_2

S_1 and S_2 are not directly known but can be obtained in terms of the compressive strengths in the two directions. This is done by reducing the biaxial failure criterion to two independent uniaxial cases. The biaxial failure criterion given by Jaeger [2] is;

$$\mu^2(C_m+a)^2 - (1+\mu^2)(\tau_m+b)^2 = S_2^2 - b^2(1+\mu^2) \qquad (B1)$$

where

C_m = mean or hydrostatic stress

τ_m = maximum shear stress

$a = S_1/\mu$

$b = S_2[\sin 2(90°-\gamma)+\mu \cos 2(90°-\gamma)]/1+\mu^2$

$= \mp S_2 \mu/1+\mu^2$ for $\gamma = 0, 90°$ respectively

Two special cases of equation (B1) are now considered, namely uniaxial compression perpendicular and parallel to the bedding plane.

First Case, $\gamma = 0$

$$C_m = \tau_m = S_{c_1}/2$$

Substituting into equation (B1)

$$\mu^2\left(\frac{S_{c_1}}{2} + \frac{S_1}{\mu}\right)^2 - (1+\mu^2)\left(\frac{S_{c_1}}{2} - \frac{S_2\mu}{1+\mu^2}\right)^2 = S_2^2 - \frac{S_2^2\mu^2}{1+\mu^2}$$

simplifying;

$$4(S_1^2-S_2^2) + 4(S_1+S_2)\mu S_{c_1} = S_{c_1}^2 \qquad (B2)$$

Second Case, $\gamma = 90°$

$$C_m = \tau_m = S_{c_2}/2$$

Substituting into equation (B1) and simplifying;

$$4(S_1^2-S_2^2) + 4(S_1-S_2)\mu S_{c_2} = S_{c_2}^2 \qquad (B3)$$

Equations (B2), and (B3) are identical to equations (16).

LIST OF REFERENCES

[1] Paul, B., and Sikarskie, D. L., "Preliminary theory of static penetration by a rigid wedge into a brittle material," Trans. AIME, 232, 372-383 (1965).

[2] Jaeger, J. C., "Shear failure of anisotropic rocks," Geological Magazine, 96, 55-72 (1960).

[3] Jaeger, J. C., Elasticity, Fracture and Flow, 2nd edition, John Wiley and Sons, Inc., 1962.

[4] Sikarskie, D. L., "Experiments on wedge indentation in rocks," Ingersoll-Rand T. N.-262, Ingersol-Rand Research Center, Princeton, New Jersey, May, 1966.

[5] Walsh, J. B., and Brace, W. F., "Fracture criterion for brittle anisotropic rock," J. Geophys. Res., 69, No. 16, 3449-3456 (1964).

[6] McLamore, R., and Gray, K. E., "The mechanical behavior of anisotropic sedimentary rocks," J. Basic Eng., Trans. ASME, 88, 62-76 (1967).

ACKNOWLEDGMENT

The authors would like to express their sincere appreciation to the Department of the Interior Bureau of Mines for the support of this work under Grant No. MIN-10.

FOOTNOTES

[1]Note that the wedge is assumed frictionless. This assumption can be removed, however, at the cost of added algebraic complexity.

[2]Other failure criteria are available, e.g. [5], including a more detailed modification of Jaeger's criterion, i.e. [6]. It is felt, however, that the added complexities of introducing a more refined failure criterion is not justified in view of the assumptions.

[3]See Appendix A for detailed algebra.

[4]A linear crushing law is assumed for convenience. Note that K, equation (10), is independent of crushing law.

[5]Note that equations (16) cannot be used for finding S_1, S_2 for $\mu = 0$.

[6]The set of roots introduced by squaring, i.e., $A^2 + B^2 = 0$, are imaginary.

TABLE I

EXPERIMENTAL DATA FOR INDIANA LIMESTONE ($2\theta = 90°$)

(Numbers in Parentheses Refers to Number of Tests Making up the Average)

γ	Compressive Strength(psi)	Crushing Slope-k(psi)	Slope of Envelope-K(psi)	Specific Energy (psi)
0°	10,900(5)	172,900(6)	58,700(3)	3,950(8)
90°	10,000(5)	154,900(4)	77,900(1)	7,220(6)

TABLE II

VALUES OF THE SHEAR CONSTANTS AS A FUNCTION OF ϕ

Shear Constants (psi)	$\phi = 5°$	$\phi = 10°$	$\phi = 20°$
S_1	5,320	4,490	3,680
S_2	2,350	1,090	460

TABLE III

NUMERICAL COMPUTATIONS

γ	Failure Angle - ψ			Slope of Envelope - K (psi)		
	$\phi = 5°$	$\phi = 10°$	$\phi = 20°$	$\phi = 5°$	$\phi = 10°$	$\phi = 20°$
0°	17.4	16.6	12.4	40,570	55,790	92,140
90°	21.6	18.0	12.8	83,900	83,160	115,630

γ	Specific Energy-Con. Rate - E_a (psi)			Spec. Energy-Con. Load - E_b (psi)		
	$\phi = 5°$	$\phi = 10°$	$\phi = 20°$	$\phi = 5°$	$\phi = 10°$	$\phi = 20°$
0°	3,560	4,990	6,910	5,650	7,280	8,420
90°	11,360	9,236	10,330	13,750	11,130	10,995

FIGURE LEGENDS

Figure 1. Bedding plane direction.

Figure 2. Incipient chip formation.

Figure 3. Constant load and other test conditions.

Figure 4. Work done in constant rate test$\left(\sum_{j=1}^{\infty} A_j\right)$; and constant load test$\left(\sum_{j=1}^{\infty} (A_j + B_j)\right)$.

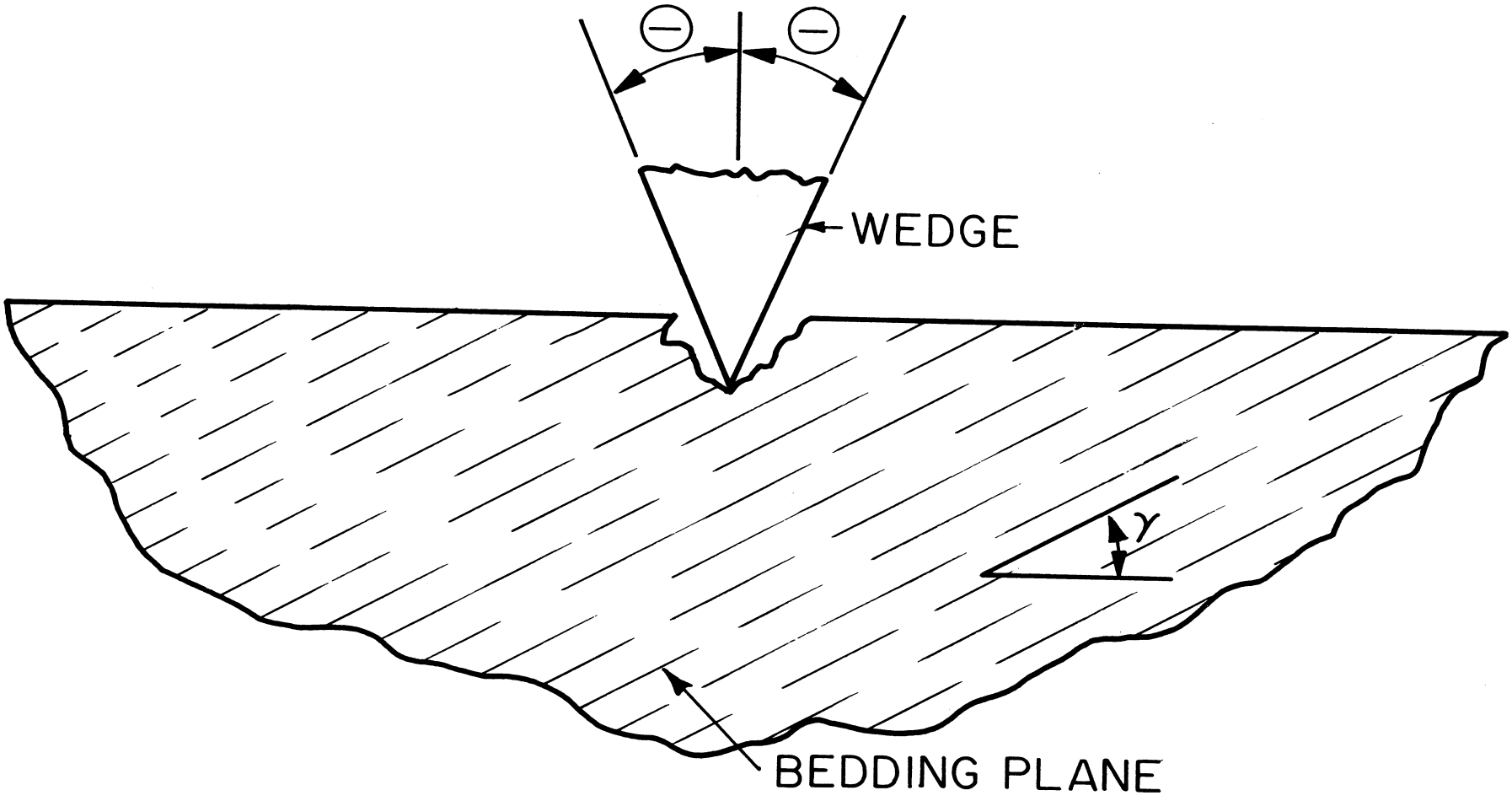

Figure 1

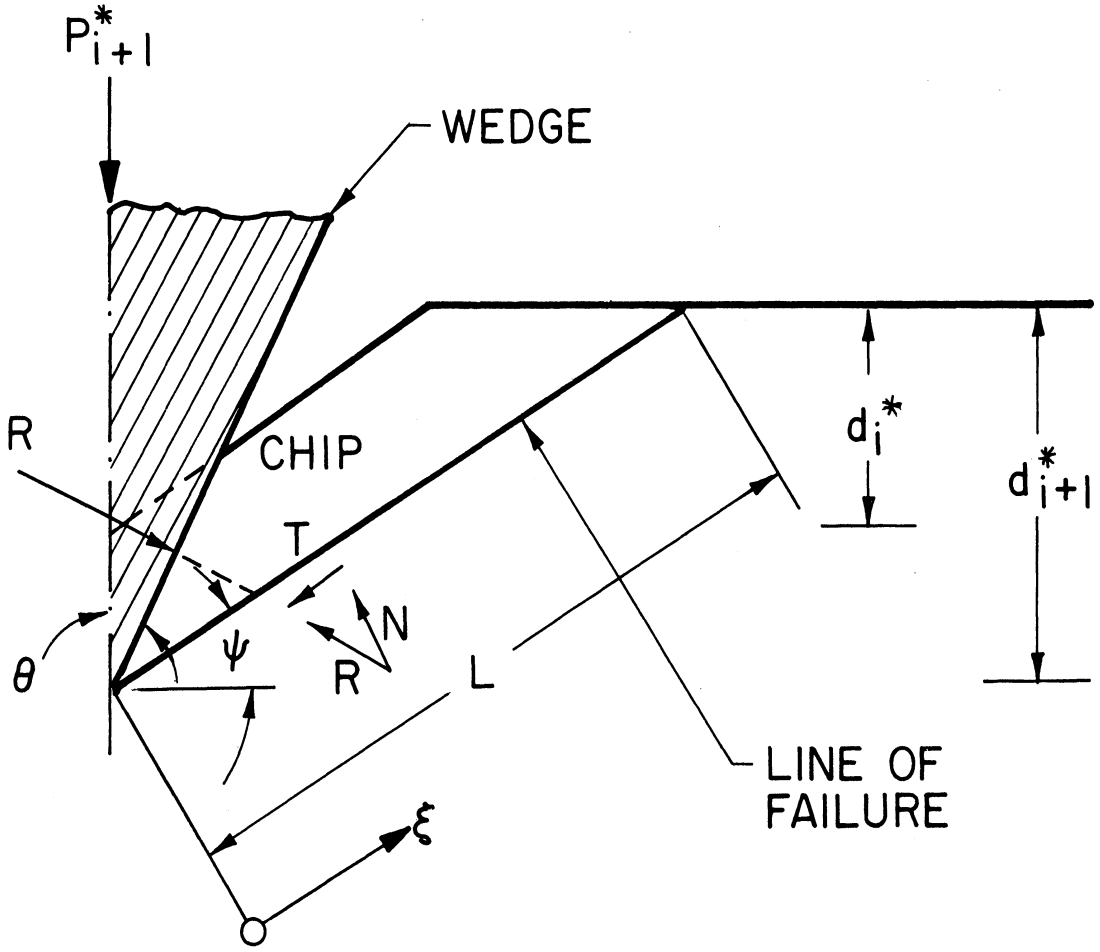

Figure 2

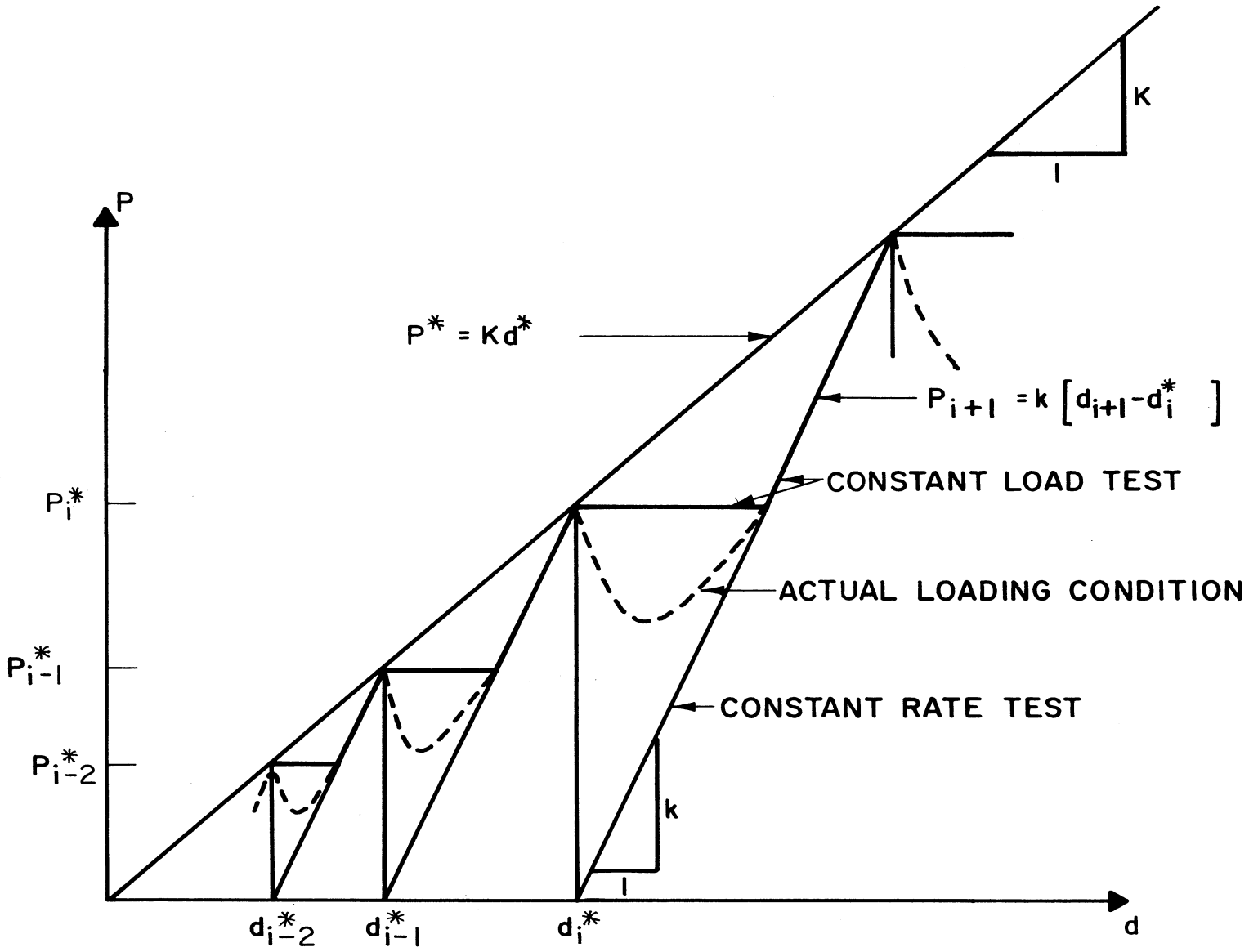
P
K
1
$P^* = Kd^*$
$P_{i+1} = k\left[d_{i+1} - d_i^*\right]$
CONSTANT LOAD TEST
ACTUAL LOADING CONDITION
CONSTANT RATE TEST
P_i^*
P_{i-1}^*
P_{i-2}^*
k
1
d_{i-2}^*
d_{i-1}^*
d_i^*
d

Figure 3

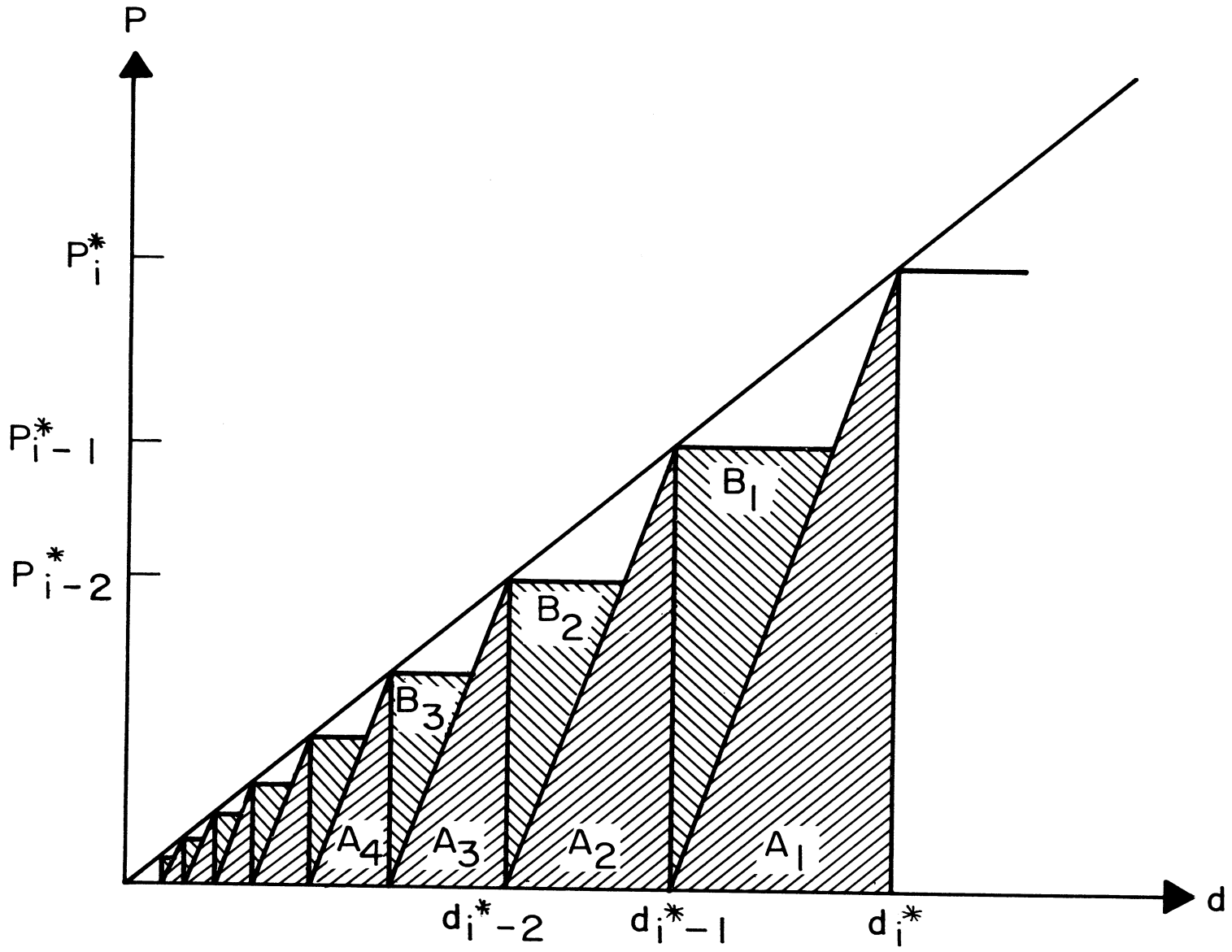

Figure 4